Biochemical and Structural Properties of Mouse Kynurenine Aminotransferase III[▽]

Qian Han,[1] Howard Robinson,[2] Tao Cai,[3] Danilo A. Tagle,[4] and Jianyong Li[1]*

Department of Biochemistry, Virginia Tech, Blacksburg, Virginia 24061[1]; Biology Department, Brookhaven National Laboratory, Upton, New York 11973[2]; OIIB, NIDCR, National Institutes of Health, Bethesda, Maryland 20892-4322[3]; and Neurogenetics, NINDS, National Institutes of Health, Bethesda, Maryland 2089-29525[4]

Kynurenine aminotransferase III (KAT III) has been considered to be involved in the production of mammalian brain kynurenic acid (KYNA), which plays an important role in protecting neurons from overstimulation by excitatory neurotransmitters. The enzyme was identified based on its high sequence identity with mammalian KAT I, but its activity toward kynurenine and its structural characteristics have not been established. In this study, the biochemical and structural properties of mouse KAT III (mKAT III) were determined. Specifically, mKAT III cDNA was amplified from a mouse brain cDNA library, and its recombinant protein was expressed in an insect cell protein expression system. We established that mKAT III is able to efficiently catalyze the transamination of kynurenine to KYNA and has optimum activity at relatively basic conditions of around pH 9.0 and at relatively high temperatures of 50 to 60°C. In addition, mKAT III is active toward a number of other amino acids. Its activity toward kynurenine is significantly decreased in the presence of methionine, histidine, glutamine, leucine, cysteine, and 3-hydroxykynurenine. Through macromolecular crystallography, we determined the mKAT III crystal structure and its structures in complex with kynurenine and glutamine. Structural analysis revealed the overall architecture of mKAT III and its cofactor binding site and active center residues. This is the first report concerning the biochemical characteristics and crystal structures of KAT III enzymes and provides a basis toward understanding the overall physiological role of mammalian KAT III in vivo and insight into regulating the levels of endogenous KYNA through modulation of the enzyme in the mouse brain.

Kynurenic acid (KYNA) is the only known endogenous antagonist of the *N*-methyl-D-aspartate subtype of glutamate receptors (6, 36, 44, 54). KYNA is also an antagonist of the α7-nicotinic acetylcholine receptor (1, 27, 43, 53). KYNA was recently identified as an endogenous ligand for an orphan G-protein-coupled receptor (GPR35) that is predominantly expressed in immune cells (57). Abnormal concentrations of KYNA have been observed in patients with multiple neurodegenerative diseases, including Huntington disease (5, 17), Alzheimer's disease (58), schizophrenia (11, 12, 52), and AIDS dementia (18). These data suggest that KYNA, acting as an endogenous modulator of glutamatergic and cholinergic neurotransmission, may play a role in the pathogenesis of these disorders. In addition to its role as an excitatory amino acid antagonist, KYNA is also involved in the control of cardiovascular function by acting at the rostral ventrolateral medulla of the central nervous system (8). Spontaneously hypertensive rats, the most widely used animal model for studying genetic hypertension, have abnormally low KYNA levels in the area of the central nervous system that tunes physiological blood pressure (29, 34).

KYNA is produced enzymatically by irreversible transamination of kynurenine, the key intermediate in the tryptophan catabolic pathway. In humans, rats, and mice, three proteins, designated kynurenine aminotransferases (KATs) I, II, and III,

are involved in KYNA synthesis in the central nervous system (16, 25, 41, 51, 60). Very recently, mitochondrial aspartate aminotransferase from rat and human brains was reported to be able to catalyze the transamination of kynurenine to KYNA and therefore was named KAT IV (15). Although the involvement of these enzymes in brain KYNA production has been discussed, their specific contributions to brain KYNA synthesis remain to be established.

Among the individual mammalian KATs, KAT I and KAT III share similar genomic structures, show high sequence identity (60), and may therefore have overlapping biological functions. In the *kat-2*$^{-/-}$ mouse brain, an increase in KAT I and KAT III expression suggests that upregulation of KAT I and KAT III may compensate for the loss of KAT II (60). These compensatory changes may also explain the rescue of hyperactivity and abnormal motor coordination in *kat-2*$^{-/-}$ mice (1, 59, 60). These studies suggest the importance of mammalian KAT I and KAT III in maintaining the KYNA level in the *kat-2*$^{-/-}$ mouse brain. Although many studies have dealt with the biochemical characteristics of mammalian KAT I and KAT II (3, 4, 9, 16, 19, 25, 49), little is known about the biochemical activity of KAT III. Likewise, the crystal structures of human KAT I (hKAT I) (48) and its homologues, glutamine-phenylpyruvate aminotransferase from *Thermus thermophilus* HB8 (13) and KAT from a mosquito, *Aedes aegypti* (AeKAT) (22), have been determined, as well as the crystal structure of hKAT II (26, 47) and its homologue from *Pyrococcus horikoshii* (7). Although KAT III has been cloned from mice, rats, and humans as a member of the mammalian KAT family (60), its structure has not been determined for any of these species. In

---

this study, we expressed mouse KAT III (mKAT III) in a eukaryotic protein expression system, purified its recombinant protein, verified its activity to kynurenine and other substrates, and determined its three-dimensional (3-D) structure and binding properties with kynurenine and glutamine. Our data provide the first biochemical and structural basis for mKAT III and form the basis for understanding its physiological functions.

MATERIALS AND METHODS

Expression and characterization of mKAT III. (i) Expression of recombinant mKAT III. Total mRNA from mouse brain was isolated using Trizol reagent (Gibco-BRL) according to the manufacturer's instructions and was used as a template for reverse transcription to produce the corresponding cDNAs. A forward primer (5′-<u>CTGCAG</u>ATGCTTTTGGCCCAGAGG-3′) containing a PstI restriction site (underlined) and a reverse primer (5′-<u>AAGCTT</u>TCAAGA CTTCTGGCTGTTCCAA-3) containing a HindIII restriction site (underlined) were used for PCR amplification of the mKAT III coding sequence (GenBank accession no. AAQ15190). The amplified cDNA fragment was cloned into a TA cloning vector and then subcloned into a baculovirus transfer vector, pBlue-Bac4.5 (Invitrogen, Carlsbad, CA), between the PstI and HindIII restriction sites. Because the signal peptide (the first 35 amino acids, encoded by exon 2) is cleaved when it is targeted to the mitochondria (37), it was not included in the expression construct. The KAT III recombinant baculovirus transfer vector was propagated in *Escherichia coli*. The cDNA insert was verified to be in frame and adjacent to the 3′ end of the polyhedron promoter by DNA sequencing. The recombinant baculovirus transfer vector was cotransfected with linearized Bac-N-Blue (*Autographa californica* multiple nuclear polyhedrosis virus) viral DNA in the presence of InsectinPlus insect cell-specific liposomes into *Spodoptera frugiperda* (Sf9) insect cells (Invitrogen). The recombinant baculoviruses were purified by a plaque assay procedure. Blue recombinant plaques were transferred to 12-well microtiter plates and amplified in Sf9 cells. Viral DNA was isolated for gene amplification analysis to determine the purity of the recombinant virus. A high-titer viral stock of a pure recombinant virus was generated by amplification in a suspension culture of Sf9 cells. The titer of the viral stock and the time course at a multiplicity of infection of 6 were established according to the manufacturer's instructions. Sf9 cells were cultured in spinner flasks in TNM-FH medium containing 10% fetal bovine serum (Invitrogen, Carlsbad, CA). KAT III recombinant virus was inoculated into the culture at a cell density of 2.5×10^6 cells/ml. Sf9 cells were harvested at day 4 postinoculation by centrifugation ($800 \times g$ for 15 min at 4°C) and then stored at −80°C until use.

(ii) Purification of recombinant mKAT III. Cell pellets were dissolved in 50 mM phosphate buffer, pH 8.0, containing 0.1% Triton X-100 and 1 mM phenylmethylsulfonyl fluoride. After sonication in cold water for 5 min, the cell lysate was centrifuged at $20,000 \times g$ for 20 min at 4°C and the supernatant was retained for mKAT III purification. Supernatant containing mKAT III was dialyzed against 20 mM phosphate buffer (pH 8.0) containing 1 mM phenylmethylsulfonyl fluoride, 0.5 mM EDTA, and 5 mM dithiothreitol and then applied to a DEAE-Sepharose column (2.5 by 20 cm). mKAT III active fractions were pooled, dialyzed against 10 mM phosphate buffer (pH 7.5) containing 5 mM dithiothreitol, and then applied to a hydroxyapatite column (1.5 by 10 cm). KAT III active fractions were eluted using a phosphate gradient (10 to 400 mM), pooled, dialyzed in 20 mM phosphate buffer (pH 8.0), and then applied to a Mono-Q column (GE Health). KAT III fractions from the Mono-Q column were concentrated using 2.0-ml membrane concentrators (with a molecular weight cutoff of 30,000). Concentrated KAT III was analyzed by gel filtration chromatography, and the collected KAT III peak was analyzed by sodium dodecyl sulfate-polyacrylamide gel electrophoresis to verify its purity.

(iii) Activity assay. The KAT activity assay was based on previously described methods (20). Briefly, a reaction mixture of 50 μl containing 5 mM L-kynurenine, 5 mM α-ketoglutarate, 40 μM pyridoxal-5′-phosphate (PLP), and 2 μg of protein sample was prepared in 100 mM boric acid buffer (pH 9.0). The mixture was incubated for 15 min at 45°C, and the reaction was stopped by adding an equal volume of 0.8 M formic acid. The reaction mixture was centrifuged at $15,000 \times g$ for 10 min, and the supernatant was analyzed by high-performance liquid chromatography (HPLC) with UV detection at 330 nm for both kynurenine and KYNA. To test the transamination activity toward other amino acids, the mixture was assayed with 10 mM amino acid, 2 mM glyoxylate or phenylpyruvate (for activity toward glycine), 40 μM PLP, 100 mM boric acid buffer, pH 9.0, and 2 μg enzyme in a total volume of 50 μl. The mixture was incubated for 15 min at 45°C

and then assayed for *o*-phthaldialdehyde thiol (OPT)-amino acid product conjugate by HPLC with electrochemical detection after the corresponding reaction mixtures were derivatized by OPT reagent (21). In the kinetic study with other amino acid substrates, a different amino acid at various concentrations (0.23 to 15 mM) and 2 mM glyoxylate in a 50-μl total volume prepared in 100 mM boric acid buffer, pH 9.0, were assayed for KAT activity. The mixture was incubated for 15 min at 45°C. To determine the substrate specificity for α-keto acids, 16 individual α-keto acids (indicated in Table 2) were tested for the ability to function as an amino group acceptor for mKAT III. In the assays, a different α-keto acid at various concentrations (0.06 to 60 mM) was used in the presence of 10 mM kynurenine, and the rate of KYNA production was determined as described for the KAT activity assay.

(iv) Effects of pH and temperature on mKAT III. To determine the effect of buffer pH on mKAT III activity, a buffer mixture consisting of 100 mM phosphate and 100 mM boric acid was prepared, and the pH of the buffer was adjusted to 6.0, 7.0, 8.0, 9.0, 10.0, or 11.0. The buffer mixture was selected to maintain a relatively consistent buffer composition and ionic strength yet to have sufficient buffering capacity for a relatively broad pH range. The reaction mixture, containing 5 mM kynurenine, 2 mM glyoxylate, and 2 μg mKAT III, was prepared using the buffer mixture at different pHs and tested for KAT activity. To determine the effect of temperature on KAT III-catalyzed kynurenine transamination, reaction mixtures in 50 μl phosphate-borate buffer (pH 9.0) were incubated at different temperatures ranging from 10 to 80°C, and the products formed in the reaction mixtures were measured by HPLC-UV analysis.

(v) Effects of other amino acids on mKAT III-catalyzed kynurenine transamination. To determine the effect of a competing amino acid on mKAT III-catalyzed KYNA production from kynurenine, an amino acid (with a final concentration of 5 mM) was incorporated into the typical reaction mixture (5 mM kynurenine, 2 mM glyoxylate, and 2 μg mKAT III in a 50-μl volume) and the enzyme activity was assayed in the same manner as that described for the KAT activity assay. The assays for each amino acid (see Table 2) were performed in triplicate, and the results were analyzed by using Student's *t* test.

Crystal structure of mKAT III. (i) mKAT III crystallization. The crystals were grown by hanging-drop vapor diffusion methods, with the volume of the reservoir solution at 500 μl and the drop volume at 2 μl, including 1 μl of protein sample (10 mg/ml) and 1 μl of reservoir solution. The optimized crystallization buffer consisted of 21% polyethylene glycol 400, 10% glycerol, 150 mM CaCl₂, and 100 mM HEPES, pH 7.5. The crystals of the glutamine-enzyme and kynurenine-enzyme complexes were obtained by soaking the mKAT III crystals in 2.5 mM glutamine and kynurenine, respectively, in the crystallization buffer for a week.

(ii) Data collection and processing. Individual mKAT III crystals were cryogenized using 15% glycerol in the crystallization buffer as a cryoprotectant solution. Diffraction data for mKAT III crystals were collected at the Brookhaven National Synchrotron Light Source beam line X29A ($\lambda = 1.0908$ Å). Data were collected using an ADSC Q315 charge-coupled device detector. All data were indexed and integrated using HKL-2000 software; scaling and merging of diffraction data were performed using the program SCALEPACK (42). The parameters of the crystals and data collection are listed in Table 1.

(iii) Structure determination. The structure of mKAT III was determined by the molecular replacement method, using chain A of the published AeKAT structure (Protein Data Bank code 1R5E) (23) without any ligands, cofactors, or waters. The program Molrep (56) was employed to calculate both cross-rotation and translation functions of the model. The initial model was subjected to iterative cycles of crystallographic refinement with Refmac 5.2 (40) and to graphic sessions for model building, using the program O (31). In the first cycles of the refinement, tight restraints on noncrystallographic symmetry were applied, but these were gradually released, and the molecules were refined independently in later stages because this gave the lowest R_{free} values. The cofactor and substrate molecules were modeled before adding solvent molecules based on both the 2Fo-Fc and Fo-Fc electron density maps when the R factor dropped to a value of around 0.24 at full resolution for the structures. Solvent molecules were automatically added and refined with ARP/wARP (45) together with Refmac 5.2. Superposition of structures was done using Lsqkab (32) in the CCP4 suite. Figures were generated using Pymol (10). Protein and substrate interactions were also analyzed using Pymol (10).

Protein structure accession numbers. The atomic coordinates and structure factors (codes 3e2f, 3e2y, and 3e2z) from this study have been deposited in the Protein Data Bank, Research Collaboratory for Structural Bioinformatics, Rutgers University, New Brunswick, NJ (http://www.rcsb.org).

TABLE 1. Data collection and refinement statistics for mKAT III crystals

Parameter	Value or description		
	mKAT III	mKAT III-Gln	mKAT III-kynurenine
Space group	P4$_3$2$_1$2	P4$_3$2$_1$2	P4$_3$2$_1$2
Unit cell			
$a = b$ (Å)	91.8	91.6	91.5
c (Å)	233.6	232.5	233.5
$\alpha = \beta = \gamma$ (°)	90.0	90.0	90.0
Data collection			
X-ray source[a]	BNL-X29	BNL-X29	BNL-X29
Wavelength (Å)	1.0809	1.0809	1.0809
Resolution (Å)[b]	2.60 (2.69–2.60)	2.26 (2.34–2.26)	2.80 (2.90–2.80)
Total no. of reflections	302,180	465,071	287,431
No. of unique reflections	32, 023	47,345	25,229
R merge[b]	0.15 (0.52)	0.09 (0.43)	0.12 (0.39)
I/s[b]	8.9 (1.1)	12.6 (1.1)	11.2 (1.6)
Redundancy[b]	10.4 (2.0)	10.3 (2.1)	11.9 (3.7)
Completeness (%)[b]	91.1 (57.4)	95.4 (64.5)	95.6 (67.3)
Refinement statistics			
R_{work} (%)	19.6	17.5	19.2
R_{free} (%)	24.6	22.1	23.7
RMS bond length (Å)	0.025	0.020	0.024
RMS bond angle (°)	2.211	1.830	2.205
No. of ligand or cofactor molecules[c]	2 LLP, 10 GOL	2 PMP, 2 Gln, 4 GOL	1 PMP, 1 LLP, 2 kynurenine, 4 GOL
No. of water molecules	140	411	83
Average B overall (Å^2)	30.5	27.8	22.6
Ramachandran plot statistics (%)			
Most favored	87.6	91.1	86.6
Allowed	12.0	8.5	13.0
Generously allowed	0.1	0.1	0.1
Disallowed	0.3	0.3	0.3

[a] BNL, Brookhaven National Laboratory.
[b] The values in parentheses are for the highest-resolution shell.
[c] LLP, lysine-pyridoxal-5′-phosphate; GOL, glycerol; PMP, pyridoxamine-5′-phosphate.

RESULTS

Enzyme purification and activity assay. Using DEAE-Sepharose, hydroxyapatite, Mono-Q, and gel filtration chromatography, we purified mKAT III recombinant protein to >98% purity, as determined by sodium dodecyl sulfate-polyacrylamide gel electrophoresis analyses. The purified mKAT III showed high KAT activity with glyoxylate as an amino group acceptor. Among the temperature points tested, mKAT III showed the highest KAT activity at 50 to 60°C (Fig. 1A). When the phosphate and borate buffer mixture, adjusted to pH 6.0 to 11.0, was used to prepare mKAT III-kynurenine-glyoxylate reaction mixtures, mKAT III displayed optimum activity around pH 9.0 to 10.0 (Fig. 1B), which is close to the optimum pH reported in the literature (3, 4, 16, 49) for mammalian brain KAT I but apparently different from the optimum pH (7.5 to 9.0) of recombinant hKAT I (25). mKAT III was tested for aminotransferase activity toward 24 different amino acids, using glyoxylate as a primary amino group acceptor. The enzyme showed activity toward a number of amino acids, including some aromatic amino acids (phenylalanine, kynurenine, tryptophan, 3-hydroxykynurenine [3-HK], and tyrosine), sulfur-containing amino acids (methionine and cysteine), and other amino acids (glutamine, histidine, asparagine, serine, alanine, aminobutyrate, and lysine) (Fig. 2). The substrate profile of mKAT III overlaps considerably with that of hKAT I (25), but hKAT I favors hydrophobic substrates and mKAT III prefers hydrophilic substrates. For example, mKAT III has high transamination activity toward asparagine, for which hKAT I has essentially no activity (25). Kinetic data provided an overview regarding the catalytic efficiency of mKAT III toward individual amino acids (Table 2). It is apparent that mKAT III is efficient in catalyzing the transamination of glutamine, histidine, methionine, phenylalanine, asparagine, cysteine, and kynurenine. Sixteen α-keto acids were tested for their potential as amino group acceptors for mKAT III, with 10 mM kynurenine as the amino group donor. Thirteen of them had detectable activity. Table 2 illustrates the enzyme kinetic parameters toward each α-keto acid, including K_m and k_{cat}/K_m. Based on kinetic analysis, glyoxylate, α-ketocaproic acid, phenylpyruvate, α-ketobutyrate, α-keto-methylthiobutyric acid, α-ketovalerate, indo-3-pyruvate, p-hydroxy-phenylpyruvate, mercaptopyruvate, and oxaloacetate are good amino group acceptors for mKAT III. Pyruvate, phenylpyruvate, and α-ketoglutarate are poor cosubstrates for the enzyme. The keto acid substrate profile of mKAT III is very similar to that of hKAT I. However, indo-3-pyruvate, which strongly inhibited hKAT I activity, showed no noticeable inhibition of mKAT III.
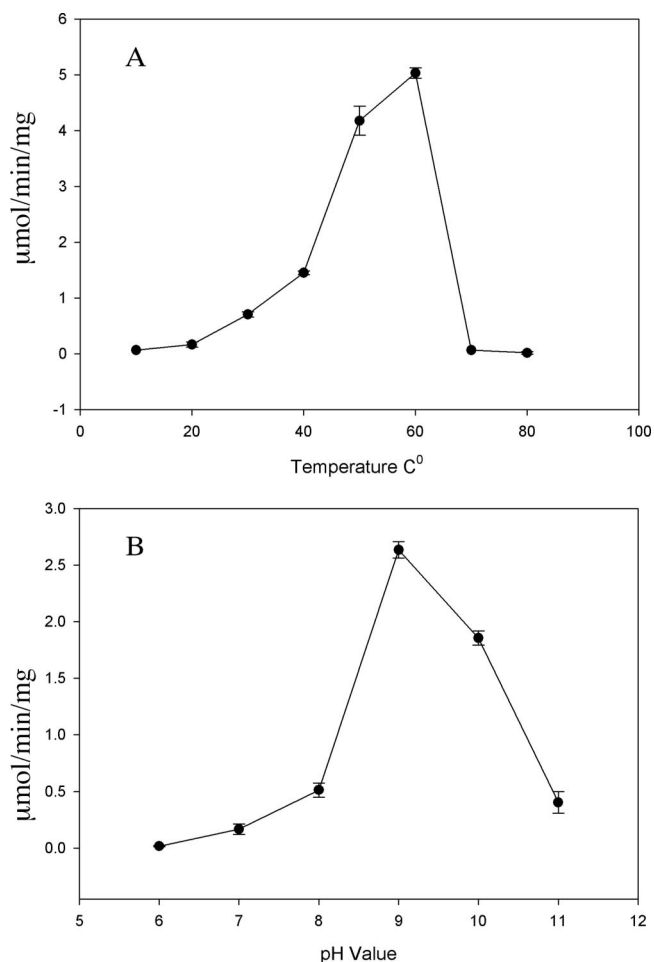
FIG. 1. Effects of pH and temperature on enzyme activity. The activities of recombinant mKAT III at different temperatures (A) and pH values (B) are shown.
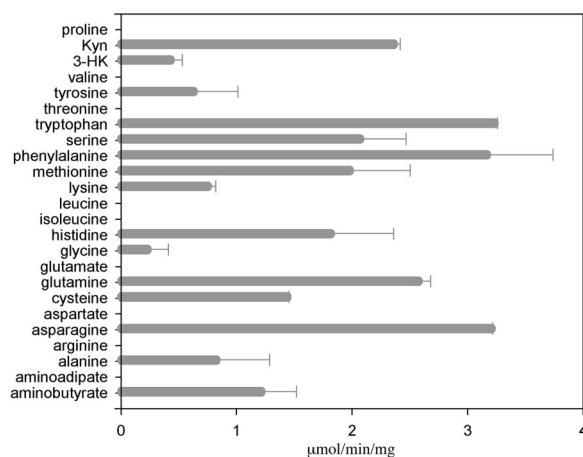

FIG. 2. Transamination activity of mKAT III toward different amino acids, with glyoxylate as an amino group acceptor. Purified recombinant mKAT III was incubated with each of the 24 amino acids at a concentration of 10 mM in the presence of 2 mM glyoxylate or phenylpyruvate (for activity toward glycine). The activity was quantified by the amount of glycine or phenylalanine produced in the reaction mixture. Kyn, kynurenine.

Overall structure. The crystal structure of mKAT III was determined by molecular replacement and refined to 2.60-Å resolution. The final model contains 2-by-410 amino acid residues and yields a crystallographic R value of 18.2% and an

Effects of other amino acids on mKAT III-catalyzed kynurenine transamination. When the typical reaction mixture (5 mM kynurenine, 2 mM glyoxylate, and 2 μg mKAT III) was assayed in the presence of each of the other amino acids (5 mM), most of the amino acids showed no noticeable effect on decreasing the rate of mKAT III-catalyzed kynurenine transamination, but the presence of cysteine, glutamine, histidine, methionine, leucine, or phenylalanine greatly decreased the rate of kynurenine transamination (Fig. 3). The decrease in the rate of KYNA production in the mKAT III–kynurenine–α-keto acid reaction mixture in the presence of different amino acids is apparently due to competitive inhibition of KAT III-catalyzed kynurenine transamination. In addition, noticeable inhibition of KAT III-catalyzed kynurenine transamination by 3-HK was also observed (Fig. 3). Although asparagine, tryptophan, serine, aminobutyrate, and lysine served as amino group donors for mKAT III, these amino acids did not seem to compete with kynurenine to inhibit KAT activity (Fig. 3). Moreover, transamination of leucine by mKAT III was not observed, but leucine effectively inhibited KAT III-catalyzed kynurenine transamination, suggesting that leucine can enter and occupy the active site of KAT III.

TABLE 2. Kinetic parameters of mKAT III toward amino acids and α-keto acids[a]

Substrate	K_m (mM)	k_{cat} (min^{-1})	k_{cat}/K_m (min^{-1} mM^{-1})
Amino acid substrates			
Glutamine	0.7 ± 0.2	136.0 ± 14.0	194.2
Histidine	0.7 ± 0.4	120.0 ± 20.0	171.4
Methionine	0.9 ± 0.7	146.0 ± 50.0	162.2
Phenylalanine	1.1 ± 0.4	162.0 ± 20.0	147.2
Asparagine	1.4 ± 0.4	176.0 ± 18.0	125.7
Cysteine	0.7 ± 0.4	78.0 ± 12.0	111.4
Kynurenine	1.5 ± 0.5	138.0 ± 18.0	92.0
Serine	3.0 ± 0.7	130.0 ± 10.0	43.3
Tryptophan	7.1 ± 4.2	213.9 ± 60.0	30.1
Tyrosine	2.7 ± 0.9	62.0 ± 8.0	23.0
Alanine	6.2 ± 2.5	92.0 ± 21.9	14.8
Keto acid substrates			
Glyoxylate	0.4 ± 0.2	162.8 ± 35.4	407.0
α-Ketocaproic acid	0.5 ± 0.2	155.3 ± 16.2	310.6
Phenylpyruvate	0.6 ± 0.3	152.0 ± 27.3	253.3
α-Ketobutyrate	1.0 ± 0.1	175.5 ± 7.4	175.5
αKMB	0.4 ± 0.2	60.9 ± 11.9	152.3
α-Ketovalerate	1.2 ± 0.3	162.2 ± 11.5	135.27
Indo-3-pyruvate	0.5 ± 0.5	62.0 ± 13.0	124.0
Hydroxy-phenylpyruvate	1.0 ± 0.1	88.9 ± 5.0	88.9
Mercaptopyruvate	2.4 ± 0.5	196.5 ± 13.6	81.9
Oxaloacetate	4.9 ± 1.2	220.7 ± 27.6	45.0
Pyruvate	10.6 ± 3.8	112.3 ± 16.9	10.6
α-Ketoisocaproic acid	5.3 ± 1.4	44.4 ± 6.3	8.4
α-Ketoglutarate	8.1 ± 12.8	22.2 ± 11.7	2.7

[a] The activities were measured as described in Materials and Methods. The K_m and k_{cat} values for keto acids were derived by using various concentrations of individual keto acids in the presence of 10 mM kynurenine; for amino acids, the data were derived by using various concentrations of individual amino acids in the presence of 2 mM glyoxylate. The parameters were calculated by fitting the Michaelis-Menten equation to the experimental data, using an enzyme kinetics module.
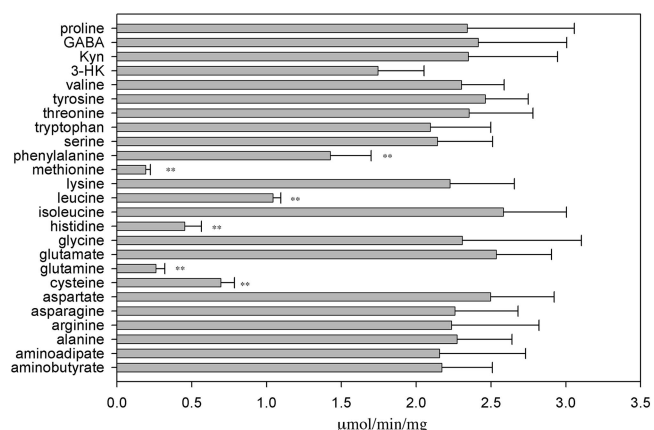
FIG. 3. Effects of various amino acids on mKAT III activity. Activities were quantified by the amounts of KYNA produced in the reaction mixtures. The rates of KYNA production in the different reaction mixtures are shown. The labeled bars (∗∗, $P < 0.01$; ∗, $P < 0.05$) show significant differences from the control. Kyn, kynurenine; GABA, γ-aminobutyric acid.

R_{free} value of 23.3%, with ideal geometry (Table 1). There are two protein molecules in an asymmetric unit which forms a biological homodimer. The residues of the two subunits in the mKAT III structure are numbered 42 to 451 for chain A and 42* to 451* for chain B (Table 1). All residues in the two subunits, except for Tyr312, are in favorable regions of the Ramachandran plot, as defined with PROCHECK (35). Although the Tyr312 residues in chains A and B fall within a disallowed region of the Ramachandran plot (Table 1) of the final model, their excellent electron densities allowed us to unambiguously assign the observed conformations.

An overview of the structure model is shown in Fig. 4A. The structure has a large domain and a small domain. The large domain (residues 80 to 335) contains a seven-stranded beta sheet, and the small domain comprises the C-terminal part and a small fragment of the N-terminal part (residues 54 to 79 and 336 to 451), which folds into a two-stranded beta-sheet covered with helices. The Asp247 residue interacts with the pyridine nitrogen of the cofactor (Fig. 4B), which is structurally and
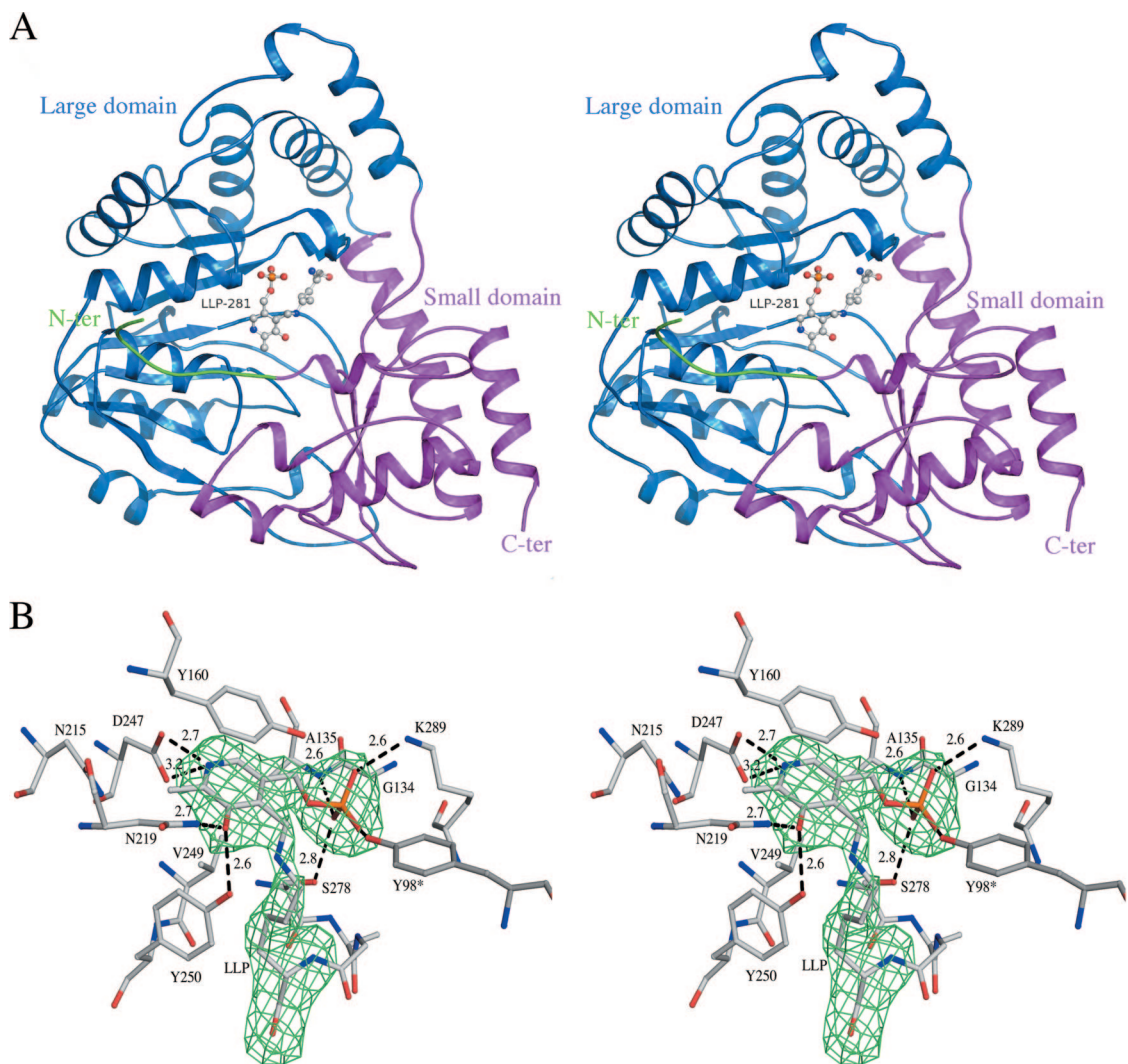

FIG. 4. (A) Stereo schematic representation of the structure of mKAT III. The small domain (pink), large domain (blue), and N-terminal arm (green) are labeled. (B) Cofactor binding site. LLP and the protein residues within a 4-Å distance of the PLP cofactor are shown as sticks. The omit map calculated without LLP is shown as an Fo-Fc electron density map contoured at the 2.8-sigma level.
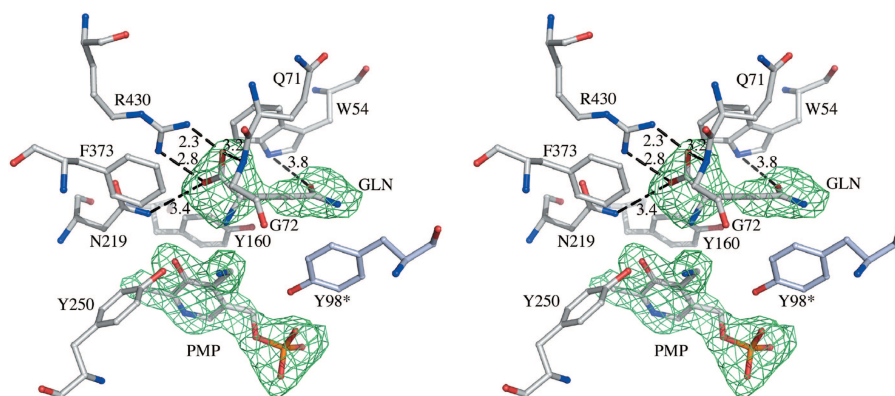
FIG. 5. PMP and protein residues within 4 Å of Gln, shown in stereo. The omit map calculated without PMP and Gln is shown as an Fo-Fc electron density map contoured at the 2.8-sigma level.

functionally conserved among fold type I PLP-dependent enzyme family members. This conservation indicates its importance for catalysis. Based on its structure, mKAT III can be considered a fold type I PLP-dependent enzyme (14, 30, 33, 38, 50).

Active site of mKAT III. Residual electron density clearly revealed the presence of covalently bound PLP in the cleft situated at the interface of the subunits in the biological dimer. The C-4A atom of PLP is covalently attached to the NZ atom of Lys281 through the formation of an internal Schiff base, and the internal aldimine gives rise to residue LLP281, represented as balls and sticks in Fig. 4B. The PLP pyridoxal ring is stacked between residues Tyr160 and Val249 by hydrophobic interactions, and the C-2A atom of PLP exhibits a hydrophobic interaction with the Asn215 side chain. The side chain of Tyr290 is hydrogen bonded to O-3 of the pyridoxal ring. The phosphate moiety of PLP is anchored by polar interactions with the peptide amide group of residues Gly134 as well as by the side chains of Tyr98* and Lys289. Most of the residues involved in PLP binding in mKAT III are identical to those involved in the PLP binding sites in hKAT I and AeKAT, except that the last two enzymes have a Phe residue in the comparable position of Tyr160 in mKAT III. A DALI-based search (28) revealed a significant structural homology of mKAT III with hKAT I (PDB code 1w7l; root mean square [RMS] deviation, 1.2 Å) (48) and AeKAT (PDB code 2r5c; RMS deviation, 1.2 Å) (23) present in the Protein Data Bank. All of these 3-D structures support the hypothesis that mKAT III is a KAT enzyme.

Substrate recognition in mKAT III-glutamine complex. The crystal structure of the mKAT III-glutamine complex was determined by molecular replacement, using the above mKAT III structure as an initial model, and refined to 2.26-Å resolution. The final model contains 2-by-410 amino acid residues and yields a crystallographic R value of 17.5% and an R_{free} value of 22.1%, with ideal geometry (Table 1). Inspection of the crystal structure of the mKAT III-glutamine complex revealed that the glutamine residue lies near the PLP cofactor, changed to its pyridoxamine-5'-phosphate (PMP) form, but that glutamine and PLP did not form an external aldimine. Several residues, including Arg430, Tyr250, Tyr160, Asn219, Phe373, Gln71, Gly72, Trp54, and Tyr98*, define the substrate-binding site and contact the glutamine molecule. The

carboxylate of glutamine forms a salt bridge with the guanidinium group of Arg430 (Fig. 5). Gln71 and Gly72 are located at the turning point of the loop that dives into and partially plugs the enzyme active site, thus shielding the substrate-binding pocket from the bulk solvents.

Substrate recognition in mKAT III-kynurenine structure. The crystal structure of the mKAT III-kynurenine complex was determined by molecular replacement, using the mKAT III-glutamine structure as an initial model, and refined to 2.80-Å resolution. The final model contains 2-by-410 amino acid residues and yields a crystallographic R value of 19.2% and an R_{free} value of 23.7%, with ideal geometry (Table 1). Similar to the case for the mKAT III-glutamine complex (Fig. 5), inspection of the crystal structure of the mKAT III-kynurenine complex revealed that kynurenine lies near the PLP cofactor in both subunits and that kynurenine and the cofactor do not form an external aldimine in any subunits, but only one cofactor was changed to PMP form in one subunit (Fig. 6A), remaining as an internal aldimine (lysine-pyridoxal-5'-phosphate [LLP]) in the other subunit (Fig. 6B). Interactive residues between kynurenine and protein are Arg430, Tyr160, Asn219, Phe373, Gln71, Gly72, Trp54, Tyr312*, and Tyr98*. The interactions are similar to those in the mKAT III-glutamine structure, but the phenyl ring of kynurenine has hydrophobic interactions with the phenyl rings of Tyr98* and Tyr312* and the indole ring of Trp54 (Fig. 6). Upon superposition of the mKAT III-glutamine structure on the mKAT III-kynurenine structure, we did not find any significant conformational changes of main protein chain and interactive residues.

Conformational change as a result of complex formation. Through superposition of all six subunits from the three mKAT III structures, we identified a major main-chain conformational change involving residues 51 to 65 in the four subunits of the KAT III-kynurenine and -glutamine complexes. Upon kynurenine or glutamine binding, the N-terminal part of the subunit moves toward and interacts with the substrate, resulting in a close interaction of Trp54 and the substrate. This conformational change also involves some side chain movement of Tyr160 and Tyr312*. In KAT III-substrate complexes, Tyr160 shifts toward the substrate and forms a hydrogen bond with the substrate (glutamine or kynurenine), and Tyr312*
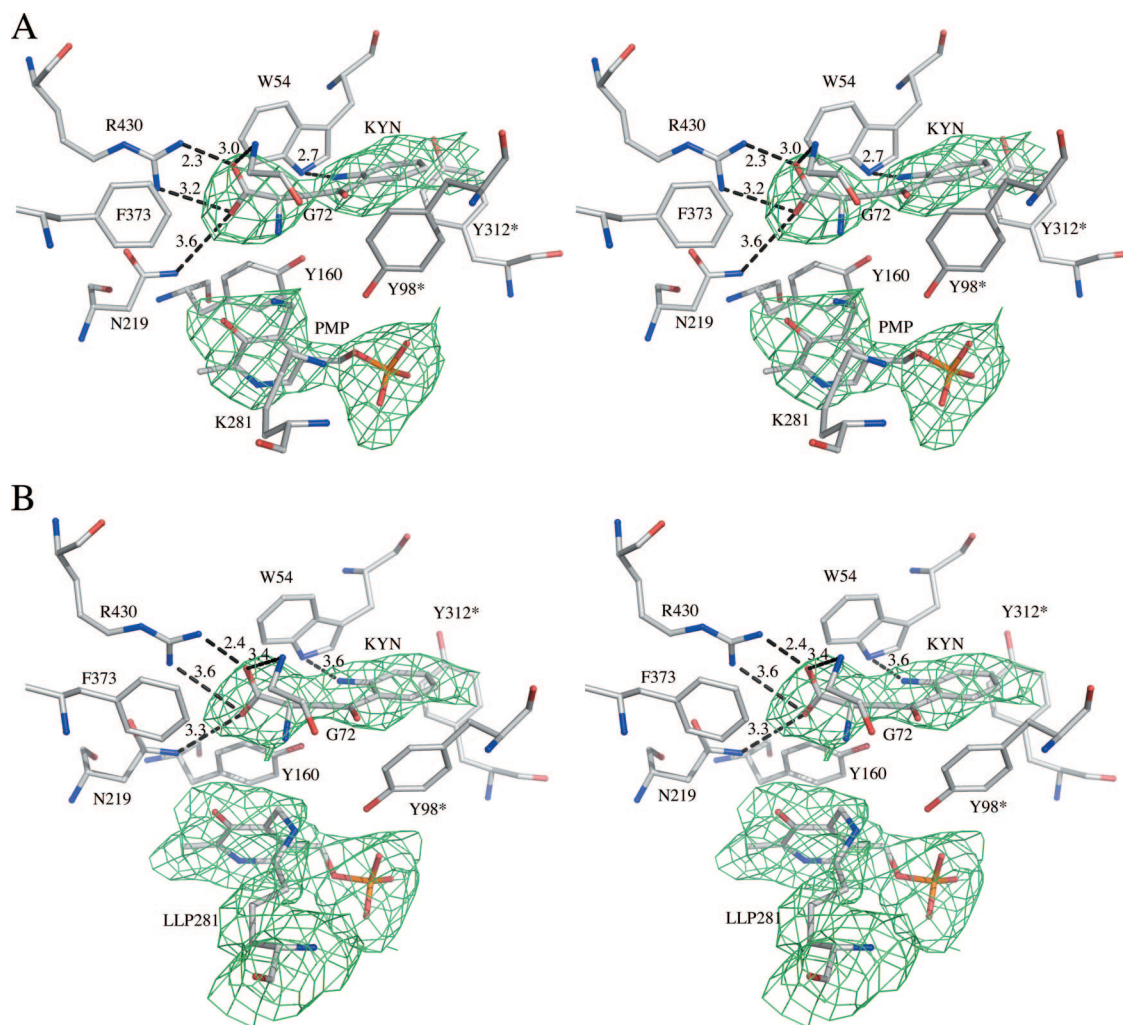
FIG. 6. PMP (A), LLP (B), and protein residues within 4 Å of kynurenine, shown in stereo. The omit map calculated without PMP, LLP, and kynurenine is shown as an Fo-Fc electron density map contoured at the 1.5-sigma level.

turns away from the center, which provides room for the substrate but maintains its interaction with the substrate (Fig. 7).

DISCUSSION

It has generally been accepted that KYNA functions as a noncompetitive antagonist of glutamatergic receptors in the mammalian brain and plays a role in alleviating potential overstimulation of the receptors by glutamate. Abnormal concentrations of brain KYNA have been implicated in several neurodegenerative diseases. KYNA, a tryptophan metabolite, is derived from kynurenine by aminotransferase-catalyzed reactions. The compound does not pass through the blood-brain barrier easily and therefore needs to be synthesized locally. Because of the close association between an abnormal concentration of brain KYNA and neurodegeneration, the enzymes involved in KYNA production are potential targets for regulating brain KYNA. However, such efforts have been hindered by the lack of detailed knowledge regarding the structure-function relationship of the mammalian KATs.

Mammalian KAT III was named based on its sequence homology with mammalian KAT I and is expressed in mammalian brains, but its biochemical and structural characteristics have never been documented at the protein level. This study demonstrates that mKAT III, expressed in a eukaryotic protein expression system, can efficiently catalyze the transamination of kynurenine to KYNA. mKAT III shows activity toward a number of amino acids, including methionine, glutamine, and histidine, and the presence of these amino acids decreases KAT III-catalyzed kynurenine transamination (Fig. 3 and Table 2). These findings are similar to those determined for hKAT I (25). An earlier report also described the inhibition of hKAT I by glutamine, phenylalanine, and tryptophan (4). It seems apparent from our results that the biochemical behaviors of KAT I and KAT III are highly similar, and consequently, it is difficult to distinguish between KAT I and KAT III activities in crude biological samples.

Critical residues related to KAT activity are conserved between KAT III and KAT I. By genetic analysis, a missense mutation (E61G) in the KAT I gene was identified in spontaneously hypertensive rats and shown to lead to reduced KAT I
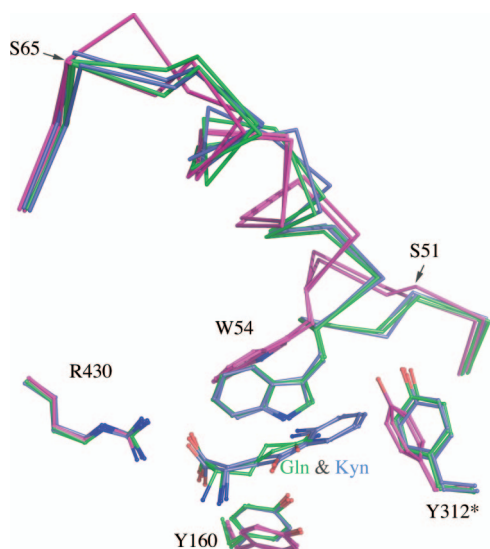
FIG. 7. Superposition of two subunits of mKAT III structure (pink), two subunits of mKAT III-kynurenine complex structure (blue), and two subunits of mKAT III-glutamine complex structure (green). N-terminal residues 49 to 67 are shown in ribbon form, and the other residues are depicted as sticks.

enzymatic activity and higher blood pressure (29, 34). Our previous study dealing with structural characterization of hKAT I revealed that the evolutionarily conserved Glu27 residue (i.e., Glu61 in the full-length sequence of KAT I), positioned at the C terminus of the H1 helix, is a pivotal residue in fixing the helix in the observed conformations. Therefore, the replacement of Glu27 with glycine in KAT I would affect the conformational change induced by substrate binding, with dramatic changes in its catalytic function (48). Interestingly, the position corresponding to the Glu27 residue is occupied by an aspartate residue in all mammalian KAT III enzymes (not shown). Structurally, aspartate is similar to glutamate, and therefore the high conservation of either glutamate in KAT I or aspartate in KAT III suggests that this position is likely essential for enzyme catalysis.

Based on the similarities of genomic structure, protein structure, and biochemical function between KAT I and KAT III, it is reasonable to speculate that KAT I and KAT III have overlapping biological functions in vivo. The high similarity of mammalian KAT I and KAT III raises the question of their origins. Evidence of gene duplication and genetic redundancy in KAT I and KAT III was first seen in the nematode *Caenorhabditis elegans*. Knockdown or knockout of either KAT I or KAT III in *C. elegans* did not result in any observable phenotypes in growth, body movements, mating, or brood size (60), which suggests functional compensation between KAT I and KAT III in nematodes.

Although mammalian KAT I and KAT III share highly overlapping biochemical properties, there are also noticeable differences between these two enzymes. The availability of highly purified recombinant hKAT I and mKAT III enabled us to critically compare the biochemical characteristics of these two enzymes. In a previous study, we determined that hKAT I was able to efficiently catalyze kynurenine to KNYA under physi-

ological conditions, but it did not show any activity toward 3-HK (25) and differed from other reports (16, 40, 49) concerning mammalian KAT I. Comparison of the pH profiles of hKAT I and mKAT III clearly indicates that mKAT III is more active than hKAT I under basic conditions. Sequence comparison revealed that KAT III from humans and mice contains more basic residues and has a higher isoelectric point than KAT I, which might be related to their differences in pH preference. For example, mKAT III has 34 lysine residues, but hKAT I shows only 24 lysine residues. The presence of 3-HK has no effect on hKAT I-catalyzed kynurenine transamination (25) but noticeably decreased mKAT III-catalyzed kynurenine transamination (Fig. 3), suggesting that 3-HK is a substrate of mKAT III. Based on these results, it seems apparent that the biochemical characteristics of mKAT III are similar to those described for mammalian brain KAT I (16, 49).

There are different optimum pH values for KAT I in the literature. Optimum pHs of 9.5 to 10 for KAT I activity were seen in isolated human brain (3, 4, 16, 49) and placenta (39), whereas optimal low pHs of 6.5 to 9 for "KAT I" activity were reported for insect cell-expressed hKAT I (pH 7.5 to 9.0) (25), rat liver (pH 6.5) (55), and heart (pH 8 to 9) (2). Since KAT I is a highly conserved protein, it is unlikely that the isolated KAT I enzyme, when tested in vitro, will have a different optimum pH. Therefore, we argue that the isolated "KAT I" enzyme with high optimal pH could potentially be KAT III.

High-alkaline and thermostable enzymes have been observed in vitro in many other cases, such as alkaline phosphatase (pH 9.5). The pH values in most living cell structures, on the other hand, are near neutrality, i.e., for the cytoplasm the pH is 6.9 and for the nucleus the pH is 7.6. It is possible that the pH required for optimum activity in vivo might not be the same as that required in vitro. Enzyme activity is usually determined using the substrate at saturating concentrations. It has been indicated that if the substrate concentration is diluted to physiological concentration, the pH optimum of the enzyme might be lowered to physiological values (46). Consequently, one has to be conscientious in judging the physiological function of an enzyme based on its in vitro optimum pH conditions. To fully understand the physiological functions of mammalian KAT I and KAT III, it is necessary to perform extensive studies of both enzymes.

The 3-D structure of mKAT III in comparison with those of hKAT I and AeKAT provides a structural basis explaining the substrate specificities of these three enzymes. We previously compared the substrate specificity of AeKAT with that of hKAT I and observed that AeKAT prefers hydrophilic substrates while hKAT I favors hydrophobic amino group donors (24, 25). Based on substrate specificity, it seems that mKAT III prefers hydrophilic substrates even more strongly than AeKAT does (Fig. 2 and Table 2) (24). Superposition of hKAT I- and AeKAT-glutamine complexes onto an mKAT III-glutamine complex shows that the three proteins have similar architectures (Fig. 8A). There are 11 residues involved in glutamine binding for the AeKAT-glutamine complex (23), and the superposition of the enzymes determined that 9 of 11 substrate-binding residues are identical in these three enzymes. The counterparts of Tyr160 in mKAT III are Phe125 in hKAT I and Tyr135 in AeKAT, and the counterparts of Tyr312 in mKAT III are Phe278 in hKAT I and Tyr286 in AeKAT (Fig. 8B).
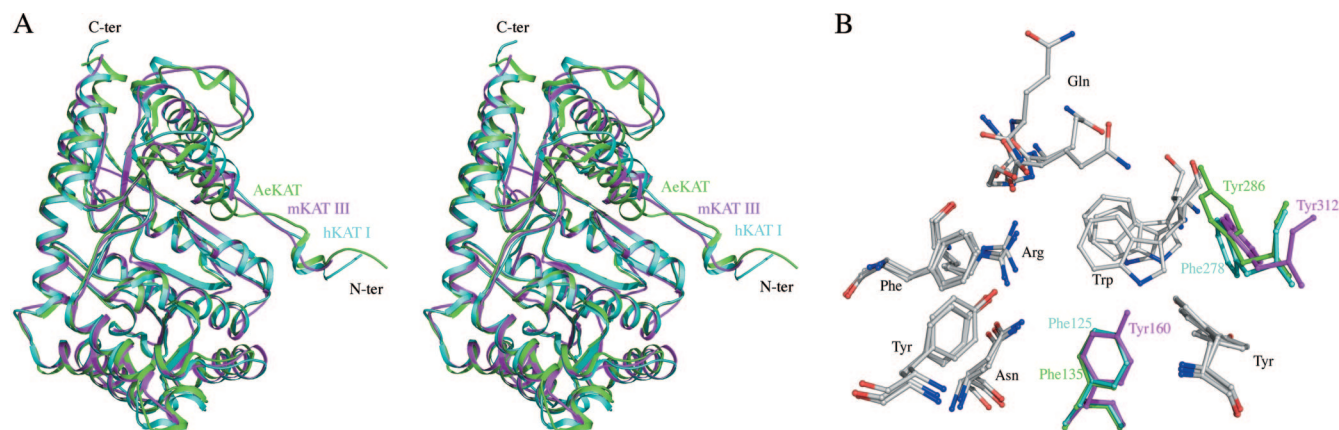
FIG. 8. (A) Stereo cartoon representation of mKAT III structure (pink), hKAT I (blue) superimposed onto mKAT III, and AeKAT (green) superimposed onto mKAT III. (B) The protein residues involved in glutamine substrate binding in the AeKAT-glutamine structure and the mKAT III-glutamine structure and the comparative residues in hKAT I are shown as sticks. Only the different residues are labeled and colored differently. The residues and ligand from AeKAT are shown in green, those from hKAT I are shown in blue, and those from mKAT III are shown in pink.

Tyrosine is less hydrophobic than phenylalanine, and the hydrophilic hydroxyl group could interact with the polar group of the amino acid donors, which likely explains the increasing preference of AeKAT and mKAT III for hydrophilic amino group donors compared with that of hKAT I.

Leucine is one of the preferred substrates of hKAT I, and it inhibits hKAT I-catalyzed kynurenine transamination at high concentrations (25). This amino acid is effective in decreasing mKAT III-catalyzed kynurenine transamination, but surprisingly, mKAT III displayed essentially no activity toward leucine. Based on its effect on decreasing mKAT III-catalyzed kynurenine transamination, leucine is apparently interactive with the enzyme, but it might not be able to position itself properly at the active site and thereby be unable to serve as a substrate. Leucine is one of the most hydrophobic amino acids. It is possible that both Tyr160 and Tyr312 in mKAT III hinder proper positioning of leucine at its active site. However, in order to clearly understand the interaction of mKAT III with leucine, it is necessary to have the structure of the mKAT III-leucine complex determined. Such structural data should be useful for the rational design of inhibitors of KAT III. In addition, the ability and inability to catalyze the transamination of leucine by KAT I and KAT III, respectively, could serve as a criterion to distinguish KAT III from KAT I activity.

In summary, this study establishes that mKAT III is able to catalyze the kynurenine-to-KYNA pathway. The 3-D structures of mKAT III and comparison of its complexes with the substrates of hKAT I and AeKAT provide insight into its preferred substrate binding and catalysis. Moreover, the similarities in biochemical characteristics of mKAT III to those reported for mammalian brain KAT I in the literature pose the possibility that the reported brain KAT I at high pH may actually be KAT III.

ACKNOWLEDGMENTS

REFERENCES

1. **Alkondon, M., E. F. Pereira, P. Yu, E. Z. Arruda, L. E. Almeida, P. Guidetti, W. P. Fawcett, M. T. Sapko, W. R. Randall, R. Schwarcz, D. A. Tagle, and E. X. Albuquerque.** 2004. Targeted deletion of the kynurenine aminotransferase ii gene reveals a critical role of endogenous kynurenic acid in the regulation of synaptic transmission via alpha7 nicotinic receptors in the hippocampus. J. Neurosci. **24:**4635–4648.
2. **Baran, H., G. Amann, B. Lubec, and G. Lubec.** 1997. Kynurenic acid and kynurenine aminotransferase in heart. Pediatr. Res. **41:**404–410.
3. **Baran, H., N. Cairns, B. Lubec, and G. Lubec.** 1996. Increased kynurenic acid levels and decreased brain kynurenine aminotransferase I in patients with Down syndrome. Life Sci. **58:**1891–1899.
4. **Baran, H., E. Okuno, R. Kido, and R. Schwarcz.** 1994. Purification and characterization of kynurenine aminotransferase I from human brain. J. Neurochem. **62:**730–738.
5. **Beal, M. F., W. R. Matson, K. J. Swartz, P. H. Gamache, and E. D. Bird.** 1990. Kynurenine pathway measurements in Huntington's disease striatum: evidence for reduced formation of kynurenic acid. J. Neurochem. **55:**1327–1339.
6. **Birch, P. J., C. J. Grossman, and A. G. Hayes.** 1988. Kynurenic acid antagonises responses to NMDA via an action at the strychnine-insensitive glycine receptor. Eur. J. Pharmacol. **154:**85–87.
7. **Chon, H., H. Matsumura, Y. Koga, K. Takano, and S. Kanaya.** 2005. Crystal structure of a human kynurenine aminotransferase II homologue from Pyrococcus horikoshii OT3 at 2.20 A resolution. Proteins **61:**685–688.
8. **Colombari, E., M. A. Sato, S. L. Cravo, C. T. Bergamaschi, R. R. Campos, Jr., and O. U. Lopes.** 2001. Role of the medulla oblongata in hypertension. Hypertension **38:**549–554.
9. **Cooper, A. J., J. T. Pinto, B. F. Krasnikov, Z. V. Niatsetskaya, Q. Han, J. Li, D. Vauzour, and J. P. Spencer.** 2008. Substrate specificity of human glutamine transaminase K as an aminotransferase and as a cysteine S-conjugate beta-lyase. Arch. Biochem. Biophys. **474:**72–81.
10. **DeLano, W. L.** 2002. The PyMOL molecular graphics system. Delano Scientific, San Carlos, CA.
11. **Erhardt, S., K. Blennow, C. Nordin, E. Skogh, L. H. Lindstrom, and G. Engberg.** 2001. Kynurenic acid levels are elevated in the cerebrospinal fluid of patients with schizophrenia. Neurosci. Lett. **313:**96–98.
12. **Erhardt, S., L. Schwieler, L. Nilsson, K. Linderholm, and G. Engberg.** 2007. The kynurenic acid hypothesis of schizophrenia. Physiol. Behav. **92:**203–209.
13. **Goto, M., R. Omi, I. Miyahara, A. Hosono, H. Mizuguchi, H. Hayashi, H. Kagamiyama, and K. Hirotsu.** 2004. Crystal structures of glutamine: phenylpyruvate aminotransferase from Thermus thermophilus HB8: induced fit and substrate recognition. J. Biol. Chem. **279:**16518–16525.
14. **Grishin, N. V., M. A. Phillips, and E. J. Goldsmith.** 1995. Modeling of the spatial structure of eukaryotic ornithine decarboxylases. Protein Sci. **4:**1291–1304.
15. **Guidetti, P., L. Amori, M. T. Sapko, E. Okuno, and R. Schwarcz.** 2007.

Mitochondrial aspartate aminotransferase: a third kynurenate-producing enzyme in the mammalian brain. J. Neurochem. **102:**103–111.

16. **Guidetti, P., E. Okuno, and R. Schwarcz.** 1997. Characterization of rat brain kynurenine aminotransferases I and II. J. Neurosci. Res. **50:**457–465.

17. **Guidetti, P., P. H. Reddy, D. A. Tagle, and R. Schwarcz.** 2000. Early kynurenergic impairment in Huntington's disease and in a transgenic animal model. Neurosci. Lett. **283:**233–235.

18. **Guillemin, G. J., S. J. Kerr, and B. J. Brew.** 2005. Involvement of quinolinic acid in AIDS dementia complex. Neurotox. Res. **7:**103–123.

19. **Han, Q., T. Cai, D. A. Tagle, H. Robinson, and J. Li.** 2008. Substrate specificity and structure of human aminoadipate aminotransferase/kynurenine aminotransferase II. Biosci. Rep. **28:**205–215.

20. **Han, Q., J. Fang, and J. Li.** 2002. 3-Hydroxykynurenine transaminase identity with alanine glyoxylate transaminase. A probable detoxification protein in Aedes aegypti. J. Biol. Chem. **277:**15781–15787.

21. **Han, Q., J. Fang, and J. Li.** 2001. Kynurenine aminotransferase and glutamine transaminase K of Escherichia coli: identity with aspartate aminotransferase. Biochem. J. **360:**617–623.

22. **Han, Q., Y. G. Gao, H. Robinson, H. Ding, S. Wilson, and J. Li.** 2005. Crystal structures of Aedes aegypti kynurenine aminotransferase. FEBS J. **272:**2198–2206.

23. **Han, Q., Y. G. Gao, H. Robinson, and J. Li.** 2008. Structural insight into the mechanism of substrate specificity of Aedes kynurenine aminotransferase. Biochemistry **47:**1622–1630.

24. **Han, Q., and J. Li.** 2004. Cysteine and keto acids modulate mosquito kynurenine aminotransferase catalyzed kynurenic acid production. FEBS Lett. **577:**381–385.

25. **Han, Q., J. Li, and J. Li.** 2004. pH dependence, substrate specificity and inhibition of human kynurenine aminotransferase I. Eur. J. Biochem. **271:**4804–4814.

26. **Han, Q., H. Robinson, and J. Li.** 2008. Crystal structure of human kynurenine aminotransferase II. J. Biol. Chem. **283:**3567–3573.

27. **Hilmas, C., E. F. Pereira, M. Alkondon, A. Rassoulpour, R. Schwarcz, and E. X. Albuquerque.** 2001. The brain metabolite kynurenic acid inhibits alpha7 nicotinic receptor activity and increases non-alpha7 nicotinic receptor expression: physiopathological implications. J. Neurosci. **21:**7463–7473.

28. **Holm, L., and C. Sander.** 1993. Protein structure comparison by alignment of distance matrices. J. Mol. Biol. **233:**123–138.

29. **Ito, S., K. Komatsu, K. Tsukamoto, and A. F. Sved.** 2000. Excitatory amino acids in the rostral ventrolateral medulla support blood pressure in spontaneously hypertensive rats. Hypertension **35:**413–417.

30. **Jansonius, J. N.** 1998. Structure, evolution and action of vitamin B6-dependent enzymes. Curr. Opin. Struct. Biol. **8:**759–769.

31. **Jones, T. A., J. Y. Zou, S. W. Cowan, and M. Kjeldgaard.** 1991. Improved methods for building protein models in electron density maps and the location of errors in these models. Acta Crystallogr. A **47:**110–119.

32. **Kabsch, W.** 1976. Crystal physics, diffraction, theoretical and general crystallography. Acta Crystallogr. A **32:**922–923.

33. **Kack, H., J. Sandmark, K. Gibson, G. Schneider, and Y. Lindqvist.** 1999. Crystal structure of diaminopelargonic acid synthase: evolutionary relationships between pyridoxal-5′-phosphate-dependent enzymes. J. Mol. Biol. **291:**857–876.

34. **Kwok, J. B., R. Kapoor, T. Gotoda, Y. Iwamoto, Y. Iizuka, N. Yamada, K. E. Isaacs, V. V. Kushwaha, W. B. Church, P. R. Schofield, and V. Kapoor.** 2002. A missense mutation in kynurenine aminotransferase-1 in spontaneously hypertensive rats. J. Biol. Chem. **277:**35779–35782.

35. **Laskowski, R. A., M. W. Macarthur, D. S. Moss, and J. M. Thornton.** 1993. Procheck—a program to check the stereochemical quality of protein structures. J. Appl. Crystallogr. **26:**283–291.

36. **Leeson, P. D., and L. L. Iversen.** 1994. The glycine site on the NMDA receptor: structure-activity relationships and therapeutic potential. J. Med. Chem. **37:**4053–4067.

37. **Malherbe, P., D. Alberati-Giani, C. Kohler, and A. M. Cesura.** 1995. Identification of a mitochondrial form of kynurenine aminotransferase/glutamine transaminase K from rat brain. FEBS Lett. **367:**141–144.

38. **Mehta, P. K., T. I. Hale, and P. Christen.** 1993. Aminotransferases: demonstration of homology and division into evolutionary subgroups. Eur. J. Biochem. **214:**549–561.

39. **Milart, P., E. M. Urbanska, W. A. Turski, T. Paszkowski, and R. Sikorski.** 2001. Kynurenine aminotransferase I activity in human placenta. Placenta **22:**259–261.

40. **Murshudov, G. N., A. A. Vagin, and E. J. Dodson.** 1997. Refinement of macromolecular structures by the maximum-likelihood method. Acta Crystallogr. D **53:**240–255.

41. **Okuno, E., M. Nakamura, and R. Schwarcz.** 1991. Two kynurenine aminotransferases in human brain. Brain Res. **542:**307–312.

42. **Otwinowski, Z., and W. Minor.** 1997. Processing of X-ray diffraction data collected in oscillation mode. Methods Enzymol. **276:**307–326.

43. **Pereira, E. F., C. Hilmas, M. D. Santos, M. Alkondon, A. Maelicke, and E. X. Albuquerque.** 2002. Unconventional ligands and modulators of nicotinic receptors. J. Neurobiol. **53:**479–500.

44. **Perkins, M. N., and T. W. Stone.** 1982. An iontophoretic investigation of the actions of convulsant kynurenines and their interaction with the endogenous excitant quinolinic acid. Brain Res. **247:**184–187.

45. **Perrakis, A., T. K. Sixma, K. S. Wilson, and V. S. Lamzin.** 1997. wARP: improvement and extension of crystallographic phases by weighted averaging of multiple refined dummy atomic models. Acta Crystallogr. D **53:**448–455.

46. **Ross, M. H., J. O. Ely, and J. G. Archer.** 1951. Alkaline phosphatase activity and pH optima. J. Biol. Chem. **192:**561–568.

47. **Rossi, F., S. Garavaglia, V. Montalbano, M. A. Walsh, and M. Rizzi.** 2008. Crystal structure of human kynurenine aminotransferase II, a drug target for the treatment of schizophrenia. J. Biol. Chem. **283:**3559–3566.

48. **Rossi, F., Q. Han, J. Li, J. Li, and M. Rizzi.** 2004. Crystal structure of human kynurenine aminotransferase I. J. Biol. Chem. **279:**50214–50220.

49. **Schmidt, W., P. Guidetti, E. Okuno, and R. Schwarcz.** 1993. Characterization of human brain kynurenine aminotransferases using [3H]kynurenine as a substrate. Neuroscience **55:**177–184.

50. **Schneider, G., H. Kack, and Y. Lindqvist.** 2000. The manifold of vitamin B6 dependent enzymes. Structure **8:**R1–R6.

51. **Schwarcz, R., and R. Pellicciari.** 2002. Manipulation of brain kynurenines: glial targets, neuronal effects, and clinical opportunities. J. Pharmacol. Exp. Ther. **303:**1–10.

52. **Schwarcz, R., A. Rassoulpour, H. Q. Wu, D. Medoff, C. A. Tamminga, and R. C. Roberts.** 2001. Increased cortical kynurenate content in schizophrenia. Biol. Psychiatry **50:**521–530.

53. **Stone, T. W.** 2007. Kynurenic acid blocks nicotinic synaptic transmission to hippocampal interneurons in young rats. Eur. J. Neurosci. **25:**2656–2665.

54. **Stone, T. W., and M. N. Perkins.** 1984. Actions of excitatory amino acids and kynurenic acid in the primate hippocampus: a preliminary study. Neurosci. Lett. **52:**335–340.

55. **Takeuchi, F., H. Otsuka, and Y. Shibata.** 1983. Purification, characterization and identification of rat liver mitochondrial kynurenine aminotransferase with alpha-aminoadipate aminotransferase. Biochim. Biophys. Acta **743:**323–330.

56. **Vagin, A., and A. Teplyakov.** 1997. MOLREP: an automated program for molecular replacement. J. Appl. Crystallogr. **30:**1022–1025.

57. **Wang, J., N. Simonavicius, X. Wu, G. Swaminath, J. Reagan, H. Tian, and L. Ling.** 2006. Kynurenic acid as a ligand for orphan G protein-coupled receptor GPR35. J. Biol. Chem. **281:**22021–22028.

58. **Widner, B., F. Leblhuber, J. Walli, G. P. Tilz, U. Demel, and D. Fuchs.** 2000. Tryptophan degradation and immune activation in Alzheimer's disease. J. Neural Transm. **107:**343–353.

59. **Yu, P., N. A. Di Prospero, M. T. Sapko, T. Cai, A. Chen, M. Melendez-Ferro, F. Du, W. O. Whetsell, Jr., P. Guidetti, R. Schwarcz, and D. A. Tagle.** 2004. Biochemical and phenotypic abnormalities in kynurenine aminotransferase II-deficient mice. Mol. Cell. Biol. **24:**6919–6930.

60. **Yu, P., Z. Li, L. Zhang, D. A. Tagle, and T. Cai.** 2006. Characterization of kynurenine aminotransferase III, a novel member of a phylogenetically conserved KAT family. Gene **365:**111–118.